Polyolefin-derived carbon nanotubes as magnetic catalysts for wet peroxide oxidation of paracetamol in aqueous solutions

Jose L. Diaz de Tuesta [a,*], Adriano S. Silva [b,c,d,e], Fernanda F. Roman [b,c,d,e], Lucas F. Sanches [b,c,f], Fernando Alves da Silva [f], Ana I. Pereira [c,g], Adrián M.T. Silva [d,e], Joaquim L. Faria [d,e], Helder T. Gomes [b,c,**]

[a] Department of Chemical and Environmental Technology, ESCET, Rey Juan Carlos University, 28933, Móstoles, Madrid, Spain
[b] Centro de Investigação de Montanha (CIMO), Instituto Politécnico de Bragança, Campus de Santa Apolónia, 5300-253 Bragança, Portugal
[c] Laboratório Associado para a Sustentabilidade e Tecnologia em Regiões de Montanha (SusTEC), Instituto Politécnico de Bragança, Campus de Santa Apolónia, 5300 253 Bragança, Portugal
[d] LSRE-LCM – Laboratory of Separation and Reaction Engineering - Laboratory of Catalysis and Materials, Faculty of Engineering, University of Porto, Rua Dr. Roberto Frias, 4200-465 Porto, Portugal
[e] ALiCE – Associate Laboratory in Chemical Engineering, Faculty of Engineering, University of Porto, Rua Dr. Roberto Frias, 4200-465 Porto, Portugal
[f] Universidade Tecnológica Federal do Paraná (UTFPR), Campus Apucarana, 86812-460 Apucarana, Brazil
[g] Research Centre in Digitalization and Intelligent Robotics (CeDRI), Instituto Politécnico de Bragança, Campus de Santa Apolónia, 5300 253 Bragança, Portugal

ARTICLE INFO

ABSTRACT

This work deals with developing feasible valorization technologies to prepare carbon nanotubes (CNTs) from plastic solid waste and demonstrate their application in catalytic wet peroxide oxidation (CWPO). CNTs were synthesized by catalytic chemical vapor deposition (CCVD) at 850 ºC, considering low-density polyethylene (LDPE), high-density polyethylene (HDPE), and polypropylene (PP) as carbon precursors representative of urban plastic solid waste. Iron oxide nanoparticles supported in alumina, previously synthesized by sol-gel, were used as catalysts in the CCVD process. TEM micrographs allow us to determine 41 nm as the average outer diameter of the CNTs and to visualize magnetic iron nanoparticles (ca. 10 nm) embedded inside the CNTs (ca. 6.4 % of content measured as ashes). These magnetic nanoparticles were kept in the CNT structure even after the purification of the CNTs with sulphuric acid, allowing to obtain magnetic CNTs. All purified and non-purified CNTs prepared from the polyolefins were assessed as catalysts in CWPO of paracetamol (PCM), used as a model pharmaceutical contaminant in water at $C_{PCM,0} = 100$ μg mL^{-1} ($C_{H2O2,0} = 472$ μg mL^{-1}, $C_{CNT} = 2.5$ g L^{-1}, $pH_0 = 3.5$ and T = 80 °C). The concentrations of PCM, H$_2$O$_2$, aromatic and total phenolic compounds were monitored for 24 h. All CNTs showed catalytic activity, allowing the complete degradation of PCM at 6 h of reaction time. The stability and reusability of materials are tested and proved in CWPO.

1. Introduction

The design of catalyst for environmental application is one of the scientific community's main concerns to develop more efficient technologies in pollution control and energy storage and conversion. For this purpose, there is special attention to developing catalysts from wastes, resulting in materials with added-value and allowing to reach the desired circular economy scenario. In addition, the manufacture cost of the catalysts can be reduced if compared to the use of purified raw materials for their preparation. In this sense, many organic wastes have been tested as a source for preparing carbonaceous catalysts (mainly hydrochars and activated carbons), such as plant residues, animal manure, sewage sludge or food waste [1–3]. As plastic solid wastes are also rich in carbon, they can serve as a source for preparing value-added carbon-based functional catalysts [4]. To date, several works have reported the synthesis and applications of plastic waste-derived carbonaceous materials. Such previous works have primarily focused on the conventional carbonization process for the preparation of amorphous

carbon phases [5,6], whereas only few examine typical carbon materials such as CNTs [7,8] or graphene [9]. Compared to biomass, polymers have well-defined structures and can yield carbonaceous catalysts with relatively well-controlled structures and content [10,11]. In addition, the controlled carbonization of synthetic polymers provides a potential mean to reutilize many plastic wastes for synthesizing carbon nano-structured catalysts [11].

Most of the studies regarding the development of CNTs from plastic wastes focus on the feasibility of CNT growth from plastic wastes and the optimization of the operating conditions. Some articles also report the application of the resulting CNTs, namely in electrochemical and energy [12–19], environmental [19–21], composite filling [22,23], and nano-medicine [24] fields. However, few studies aim to tune the development of CNTs with suitable characteristics for catalytic processes or other applications. In contrast, most studies report methods to tune the nanostructure carbon catalysts post-production to obtain the desired properties of the material by functionalization with heteroatoms [25] or by impregnation with an metal active phase [26–28]. Latter is the case of carbon materials doped with iron-based compounds to confer magnetic properties. However, the method most used for synthesizing of CNTs consists in the catalytic chemical vapor deposition (CCVD) over metal substrates typically based on iron or cobalt [9,29]. Bearing this in mind, a novel approach will be the production of CNT by CCVD on substrates, which allow to directly obtain CNTs with magnetic properties, avoiding a subsequent process to impregnate the CNT with magnetic materials.

The application of magnetic nanostructured carbon materials has received special interest in Fenton-like systems or catalytic wet peroxide oxidation (CWPO), due to the inherent catalytic activity of magnetic iron-based catalysts and enabling in-situ magnetic separation from the media of reaction [30]. The CWPO process is a technology used for the treatment of wastewater, in which the degradation of organic pollutants goes through hydrogen peroxide-assisted oxidation in the presence of a suitable catalyst under mild operating conditions (preferably at 1 bar and 25–80 ºC) [31,32]. CNTs have been found as exceptional catalysts leading to high removals of the organic matter present in wastewater effluents by CWPO [30,33–37]. As a novel approach, recent studies report the application of CNTs impregnated with magnetite to confer the above-mentioned magnetic properties and enable the in-situ separation by magnetism [26–28]. The magnetite-CNTs were applied in the removal of naproxen, diclofenac and ibuprofen, and the great potential of CWPO with magnetic catalysts based on CNTs for the abatement of micro-pollutants was demonstrated.

This work deals with synthesizing CNTs from polyolefins (PO-CNTs) by CCVD over an iron-based substrate as a novel approach to produce in-situ magnetic CNTs using carbon sources representative of plastic wastes. Upon the acquired magnetism, the PO-CNTs will prove their adequacy in CWPO, with the added advantage of being easily recovered from the treated solutions by applying a magnetic field. As representative polymers of plastic wastes, LDPE, HDPE and PP are explored as carbon-rich feedstocks to prepare CNTs. CCVD was performed using iron oxide supported on alumina as a catalyst to confer magnetic properties to the CNTs, which were kept even after their purification with sulphuric acid because of the encapsulation of metallic nanoparticles within the CNT structure. Then, the purified and non-purified PO-CNTs are explored in CWPO of PCM, used as model micro-pollutant.

2. Methodology

2.1. Reagents and materials

The precursors used in the preparation of the CNTs, namely HDPE (melt index 2.2 g (10 min)$^{-1}$), LDPE (average Mw $\sim$ 35,000 g mol^{-1}, average Mn $\sim$7700) and PP (average Mw $\sim$250,000 g mol^{-1}, average Mn $\sim$67,000), were supplied by Sigma-Aldrich. For the preparation of the supported magnetic nanoparticles, iron (II) chloride tetrahydrate (98 %), iron (III) chloride hexahydrate (97 %), absolute ethanol (99.8

%), and ethylene glycol (99 %), obtained from Acros Organics, VWR Chemicals, Fisher Chemical and Fisher Chemical, respectively, were used. Alumina was supplied by BASF in pellets form. Prior to use, it was ground and sieved (53–106 μm). In CWPO runs, paracetamol (98 %) and hydrogen peroxide (30 %), supplied by Alfa Aesar and VWR Chemicals, were used. Sulphuric acid (95 %) from VWR Chemicals was used for CNTs purification purposes. For analytical measurements, orthophosphoric acid (85 %), sodium sulphite anhydrous (98 %), titanium (IV) oxysulfate (99.99 wt % metal basis, c.a. 15 wt % solution in dilute sulphuric acid), Folin-Ciocalteu's reagent and gallic acid anhydrous provided by Fisher Chemical, Panreac, Sigma Aldrich, PanReac, Merck, were used. All chemicals were used as received. Ultrapure and distilled water were used to prepare solutions and for washing procedures during this work.

2.2. Synthesis of PO-CNTs catalysts

PO-CNTs were synthesized by the CCVD process growing on ferromagnetic nanoparticles supported on alumina. The preparation of the ferromagnetic nanoparticles was performed through the sol-gel method. First, two solutions of 20 mL of ethanol with 10 mmol of FeCl$_2$·4 H$_2$O and 80 mL of ethylene glycol with 20 mmol of FeCl$_3$·6 H$_2$O were stirred and heated at 80 °C and 60 ºC, respectively, and then cooled to room temperature. Both solutions were mixed with 6.6 g of alumina, stirred, and the resultant mixture was heated to 60 °C for 2 h, then heated to 120 °C until a gel texture was achieved, and finally to 210 °C until a dry powder was obtained. The powder synthesized was calcined at 300 °C for 12 h and at 600 °C for 24 h in air atmosphere, to obtain iron oxide (IO) over alumina, labelled as IO/Al$_2$O$_3$ catalyst.

For the CCVD process, the reactor set-up shown in Fig. 1 was used. The reactor is equipped with 2 crucibles, wherein the first crucible was loaded with 5 g of polyolefin (LDPE, HDPE and PP), and the second crucible with 1 g of the magnetic catalyst (IO/Al$_2$O$_3$). The working temperature was 850 °C for 1 h with N$_2$ flow of 50 mL min^{-1}. The synthetized nanotubes were labelled as CNT_LDPE, CNT_HDPE and CNT_PP, according to the polymer used.

Each CNT produced was purified to remove the remaining IO/Al$_2$O$_3$. For this purpose, 1 g of CNT and 50 mL of H$_2$SO$_4$ (50 %) were stirred and heated to 140 °C during 3 h. The solid was recovered through filtration and washed with distilled water until the rinsing water reached the pH of the distilled water. Finally, the CNTs were dried for 12 h at 60 °C in an air atmosphere. The washed nanotubes were named as CNTW_LDPE, CNTW_HDPE, and CNTW_PP, respectively, according to the polymer used in their preparation.

2.3. Characterization techniques

JEOL 2100 high-resolution transmission electron microscope (HR-TEM) with LaB6 filament operating at 200 kV was used to obtain the microphotographs of the CNTs.

The textural properties of the materials were determined from N$_2$ adsorption–desorption isotherms obtained at − 196 °C in a Quantachrome NOVATOUCH XL4 adsorption analyzer, following the same procedure as described elsewhere [38]. Briefly, the degasification of the catalysts was conducted at 120 ºC during 16 h and then adsorption isotherms were obtained. Afterwards, BET (S_{BET}) was determined using the BET method, and total pore volume (V_{Total}) was determined at p/p^0 = 0.98. Calculations of those methods were all done using TouchWinTM software v1.21.

Elemental analysis of the PO-CNTs was performed using a CHNS analyzer Flash 2000 (Thermo Fisher Scientific, Massachusetts, USA), equipped with a thermal conductivity detector to quantify the carbon, hydrogen, nitrogen and sulfur contents.

The thermogravimetric analyses (TGA) of the PO-CNTs materials were conducted under air atmosphere in a Diamond TG/DTA (TG 209F3, NETZSCH) apparatus heating from 50 to 850 ºC at 10 ºC min^{-1}.
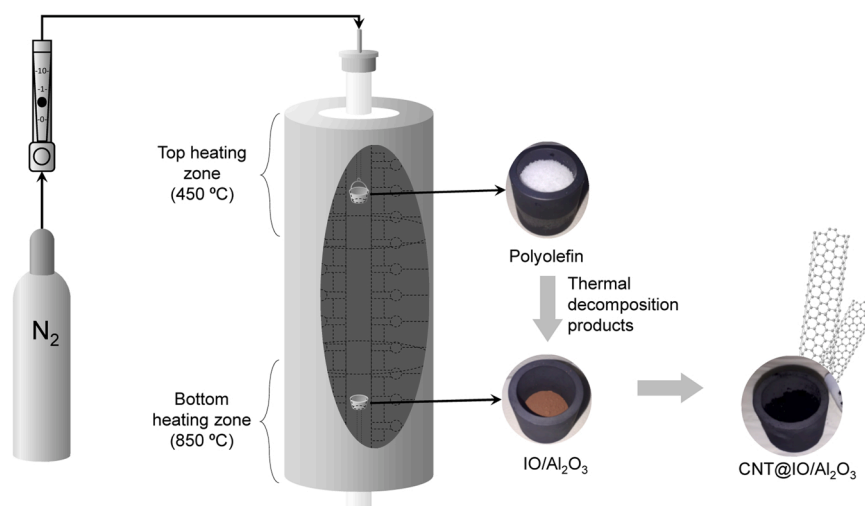
Fig. 1. Experimental setup used for the synthesis of carbon nanotubes (CNTs) by sequential thermal decomposition of the polyolefins and catalytic chemical vapor deposition (CCVD) over the prepared magnetic substrate (IO/Al₂O₃).

The ash percentage of the PO-CNTs was determined by adapting the methodology presented elsewhere [39]. Briefly, PO-CNTs were burnt in a muffle at 550 °C until a constant mass was reached in a precision balance (± 0.0005 g).

The percentage of iron in CNTs samples was determined upon digestion of the samples (15 mg) with *aqua regia* (10 mL) at 200 °C for 6 h under autogeneous pressure in an autoclave. The resulting liquid was collected and filtered (0.45 μm) and diluted with 5 % HNO₃ solution. The concentration of Fe was determined via atomic absorption (Pinaacle 900 T, Perkin Elmer).

X-ray diffraction (XRD) analyses were made, at room temperature, with a PANalytical X′Pert Pro diffractometer, equipped with X′Celerator detector and secondary monochromator in θ/2θ Bragg-Brentano geometry. The measurements were carried out using 40 kV and 30 mA, a CuKα radiation ($\lambda\alpha_1$ = 1.54060 Å and $\lambda\alpha_2$ = 1.54443 Å), 0.017°/ step, 100 s/step, in a 10–80 ° 2θ angular range.

2.4. CWPO experiments

Both purified and non-purified PO-CNTs were tested as catalysts (2.5 g L⁻¹ of catalyst load) in the CWPO of 100 μg mL⁻¹ paracetamol (at initial pH (pH_0) adjusted to 3.5), 80 ºC and using the stoichiometric quantity of H₂O₂ for the complete oxidation of 100 μg mL⁻¹ of paracetamol, according to the following chemical reaction:

$$C_8H_9NO_2 + 21H_2O_2 \rightarrow 8\ CO_2 + 25H_2O + HNO_3$$
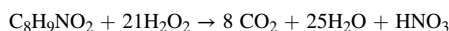
Therefore, the concentration of hydrogen peroxide was established at 472 mg L⁻¹. Procedure and monitorization were conducted as described in previous works [40]. Briefly, samples were collected at selected times for the analysis of the PCM, TOC, aromaticity, phenol, and H₂O₂ concentrations. PCM concentration was determined by using a Jasco HPLC with a UV–VIS detector at a wavelength of 277 nm, the H₂O₂ concentration was monitored by colorimetric analysis with TiOSO₄, and the total organic carbon (TOC) content was determined using a Shimadzu TOC-L CSN analyzer [40]. After the reaction, the PO-CNT spent catalyst was washed with distilled water and dried in air oven at 60 °C for 24 h to recover the catalyst and perform additional CWPO runs to check its reusability.

Selected experiments were performed in triplicate to assess reproducibility and error of the experimental results. In addition, the non-catalytic peroxide oxidation of paracetamol was conducted to observe the possibility of non-catalytic contribution to its degradation. Furthermore, adsorption tests were conducted with all PO-CNTs at the same conditions tested in the CWPO of paracetamol (2.5 g L⁻¹ of PO-

CNT as adsorbent, 100 μg mL⁻¹ of paracetamol, pH_0 = 3.5 and 80 °C), but in the absence of H₂O₂.

The concentrations of aromatic compounds formed during CWPO were quantified using a method described elsewhere [28]. The analysis consists in the dilution of 0.5 mL of the sample with a buffer solution of H₃PO₄ at pH 7. Thereafter, the aliquot was analysed in a UV–VIS spectrophotometry Jasco V-530 equipment at the wavelength of 254 nm.

The presence of intermediates as total phenolic compounds was determined by adapting the Folin-Ciocalteu's reagent (FCR) methodology presented in the literature [28,41]. Briefly, 0.5 mL of the sample was added into 0.5 mL of the FCR with 2 mL of distilled water, and 0.35 mL of an aqueous solution of Na₂CO₃ 10 % (w/v). After that, Na₂CO₃ was added, the aliquot was left to rest for 1 h and then absorbance was determined by UV–VIS spectrophotometry (Jasco V-530) at the wavelength of 765 nm. The concentration of the total phenolic compounds in the sample was determined using gallic acid as a phenolic compound model.

Aliquots at the end of the oxidation runs were taken and analyzed by atomic absorption (Pinaacle 900 T, Perkin Elmer) to observe whether iron was leached from CNTs into the aqueous media of reaction.

2.5. Calculation methods

The efficiency of H₂O₂ consumption (η_{H2O2}) was defined according to the quantity of H₂O₂ needed to completely oxidize 1 mol of C to CO₂, generating H₂O as subproduct, as indicated in Eq. (1):

$$C + 2H_2O_2 \rightarrow CO_2 + 2H_2O \tag{1}$$

Therefore, η_{H2O2} was determined by Eq. (2) [42]:

$$\eta_{H_2O_2,6h}(\%) = \frac{n_{TOC,0} - n_{TOC,6h}}{n_{H_2O_2,0} - n_{H_2O_2,6h}} \cdot \left(\frac{2\quad mol_{H_2O_2}}{1 mol_{TOC}} \right) \cdot 100 \tag{2}$$

where $n_{TOC,0}$ and $n_{H_2O_2,0}$ refer to the mole quantity of TOC and hydrogen peroxide at the beginning of the reaction; and $n_{TOC,6h}$ and $n_{H_2O_2,6h}$ are those quantities after 6 h of reaction time, respectively.

The conversion of PCM, either by adsorption ($X_{PCM,ADS}$) or by CWPO ($X_{PCM,CWPO}$), the abatement of TOC (X_{TOC}), and the removal of aromatic (X_{AROM}) and total phenolic compounds ($X_{phenols}$) were calculated as described in Eq. (3):

$$X_i = \frac{C_{i,0} - C_i}{C_{i,0}} \tag{3}$$

where $C_{i,0}$ and C_i refer to the PCM, TOC, aromatic and total phenolic

compounds concentrations at the beginning of the reaction and at a specified time, respectively.

3. Results and discussion

3.1. Morphology of the PO-CNTs

The same catalyst, based on iron oxide over alumina, was tested to promote the CNT growth by CCVD from different polyolefins, used as carbon feedstocks precursors, and further purified with H_2SO_4 to remove the remaining metal substrate. The morphology of the purified PO-CNTs prepared from polyolefins was investigated by TEM analysis (Fig. 2). As observed, all PO-CNTs belong to a type of multi-walled fibrous structures with hollow cavities, allowing to conclude about the feasibility of employing the magnetic substrate as a catalyst for the growth of CNTs from LDPE, HDPE and PP, as carbon precursors. The nanotubes are not straight, and cup-stacked or bamboo-like structures are observed in the micrographs of CNTW_LDPE (a-c), CNTW_HDPE (d-f) and CNTW_PP (g-i). The outer diameters observed among all the micrographs taken were determined as 37 ± 12, 44 ± 24 and 43 ± 23 nm

for CNTW_LDPE, CNTW_HDPE, and CNTW_PP, respectively. In the same order, the thickness of the PO-CNTs was found to be 28 ± 3, 33 ± 5, and 35 ± 2 nm. The high resolution of the microphotographs allowed to determine the graphene layers forming the nanotubes that were found to range from 14 to 37 layers (17 layers are presented in Fig. 2.i). As observed, the different precursors used do not significantly affect the inner-outer diameters of the PO-CNTs obtained.

The diameters achieved in the polyolefins-derived CNTs of this work are smaller than other CNT prepared from plastics found in the literature: of about 56 nm [43], 60 nm [44], 80 nm [45], or 160 nm [46].

As can be noted, all PO-CNTs present a nanoparticle embedded inside the tubes, regardless of the polyolefin precursor used as feedstock for their synthesis. The size of the nanoparticles observed in the PO-CNTs is close to 13 ± 6 nm (a particle with a size of 6 nm can be observed in Fig. 2.i). The elemental mapping (Fig. 2.b, c and e) shows that PO-CNTs and the embedded nanoparticles are composed only by carbon and iron, respectively. The iron nanoparticles are expected to come from the substrate used in the growth of the CNTs, revealing that CNTs grow taking the IO nanoparticles from alumina support. It is noteworthy that iron nanoparticles are also observed after the
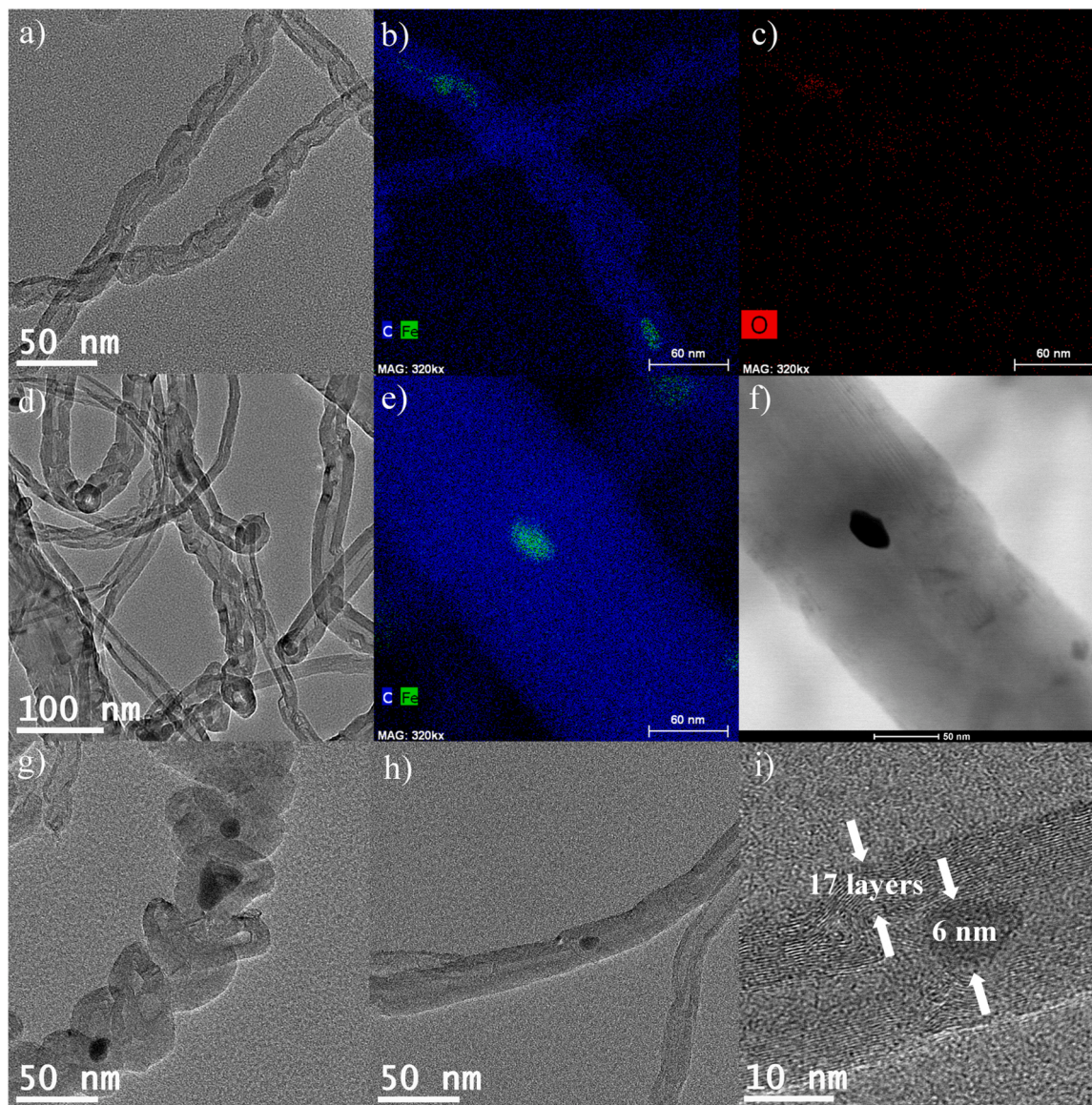

Fig. 2. TEM micrographs of the purified carbon nanotubes (CNTWs) obtained by chemical vapor deposition (CCVD) over IO/Al$_2$O$_3$ from using (a-c) LDPE, (d-f) HDPE and (g-i) PP as carbon feedstock.

purification step with H_2SO_4 (implemented to remove attached metal species arising from the CCVD system).

3.2. Thermogravimetric analysis of the PO-CNTs

Fig. 3 represents the mass losses of the purified PO-CNTs prepared from LDPE, HDPE and PP, determined by TGA under air atmosphere from 50 to 850 ºC, with a heating ramp of 10 ºC min^{-1}. As observed, the purified PO-CNTs present the main mass losses centered at 648, 647 and 640 ºC for CNTW_LDPE, CNTW_HDPE and CNTW_PP, respectively. This denoted a high resistance to oxidation, as also found in other ordered structured carbon-based materials, as graphite [47], diamond [48] or graphene [49]. This resistance to oxidation is consistent with the proposed structures of these nanometer-sized materials, in which aromatic bonding dominates and dangling bonds are minimal [47]. The mass losses start to be significant close to 530–560 ºC and the CNTs are completely burnt at ca.720 ºC, regardless of the carbon feedstock used in its preparation. The burn of the material takes those ranges, because only sites on the outermost graphene layer of the CNTs are accessible to oxygen. Since these sites are relatively rare compared to the bulk of the carbon in inner layers and in unstrained structures, these CNTs are remarkably resistant to oxidation. As TGA-derivative curve profiles are composed of just one narrow peak, it is possible to conclude that CNTs are composed by a well-defined structure [33].

The content of ashes in the purified PO-CNTs ranged from 5.6 % to 7.7 %. These ashes content refer to the iron nanoparticles embedded inside the PO-CNTs, which may be observed in the TEM microphotographs. More details about the composition and ashes content of the nanotubes are described in the following section.

3.3. Elemental composition and textural properties

Table 1 summarizes the elemental composition (N and S-contents being negligible), ash content, and the textural properties of the polyolefins-derived CNTs prepared over the iron/alumina substrate. As can be noted, the purified carbonaceous materials (CNTW_LDPE, CNTW_HDPE, and CNTW_PP) show high carbon contents in their composition (92.5, 94.0 and 92.0 wt %, respectively). The percentages of carbon are higher than in their respective non-purified materials (58.3, 59.5, and 62.2 wt % in CNT_LDPE, CNT_HDPE, and CNT_PP, respectively) due to the significant removal of metals, as a consequence of the treatment with sulphuric acid for their purification, as demonstrated by the ash content in the PO-CNTs.

The yield obtained in the CCVD process under study range from 41.9 to 47.6 wt %, measured as the weight percentage of CNTs per weight percentage of polyolefin. Ash content decreases from 38.2, 39.8, and 35.0 wt % for CNT_LDPE, CNT_HDPE and CNT_PP to 6.0, 5.6, and 7.7 wt % for CNTW_LDPE, CNTW_HDPE, CNTW_PP, respectively. Part of these ashes are due to the iron content. The amount of iron in PO-CNTs samples, obtained by atomic absorption analysis of the digested PO-CNTs, is shown in Fig. 4. As observed, iron content in polyolefin-derived nanostructured carbon materials before the purification procedure is in the range of 7.6–9.4 wt %. The highest amount of iron is present in PO-CNTs prepared using LDPE and HDPE as carbon sources (9.3 and 9.4 wt %, respectively), followed by PP (7.6 wt %). For the purified samples, the range of iron percentage decreased to 2.4–4.8 wt %, representing a decrease in the iron content of about 37–74 wt %, depending on the precursor. According to these values, the percentage of iron content in ashes is 24.3, 23.6 and 21.7 wt % for non-purified PO-
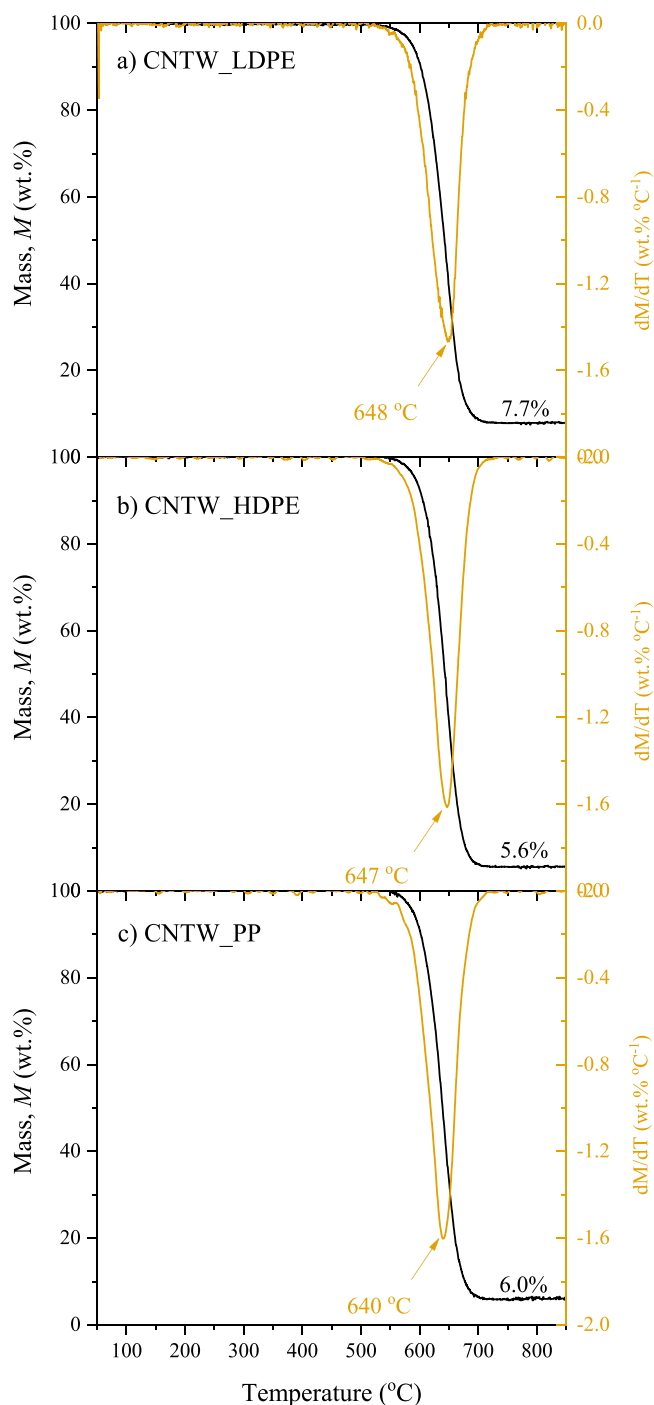

Fig. 3. Mass losses (left Y-axis) and their corresponding derivatives (right Y-axis) of PO-CNTs prepared from a) LDPE, b) HDPE and c) PP feedstocks.

Table 1
CHNS-Elemental analysis[a], ash content and textural properties of the PO-CNTs.

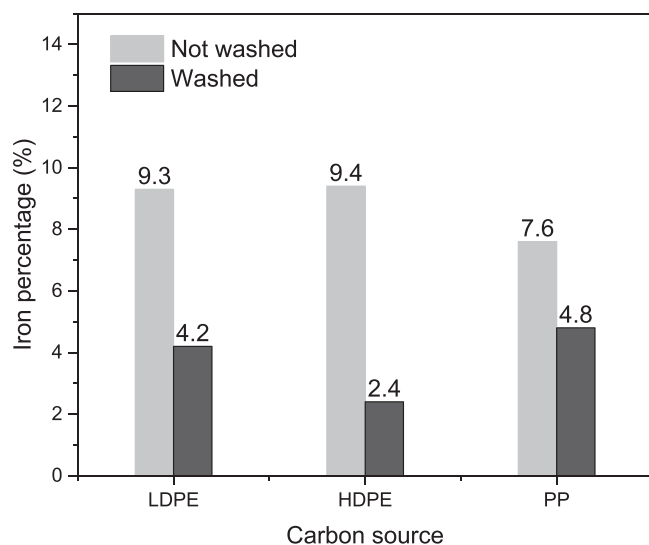| Material	C (wt %)	H (wt %)	Ash content (wt %)	S_{BET} (m^2 g^{-1})	V_{Total} (mm^3 g^{-1})
CNTW_LDPE	92.5 ± 0.9	0.19 ± 0.22	6.0 ± 0.2	66	172
CNTW_HDPE	94.0 ± 0.5	0.14 ± 0.04	5.6 ± 0.2	75	184
CNTW_PP	92.0 ± 0.7	0.10 ± 0.01	7.7 ± 0.1	94	247
CNT_LDPE	58.3 ± 2.3	0.21 ± 0.01	38.2 ± 1.4	67	154
CNT_HDPE	59.5 ± 2.3	0.19 ± 0.01	39.8 ± 1.2	80	215
CNT_PP	62.2 ± 3.9	0.23 ± 0.02	35.0 ± 1.5	98	244
IO/Al$_2$O$_3$	-	-	-	139	326
Al$_2$O$_3$	-	-	-	185	437

[a] N and S-contents are negligible.

Fig. 4. Iron percentage in CNTs prepared using different polyolefin carbon sources.

CNTs (CNT_LDPE, CNT_HDPE, and CNT_PP, respectively) and increase to 70.0, 42.9, and 62.3 wt % for CNTW_LDPE, CNTW_HDPE, CNTW_PP, respectively. This means that the treatment with sulphuric acid was efficient in purifying CNTs, removing the metal content, and mainly the alumina support. The quantity of iron present in IO/Al_2O_3 was also measured by atomic absorption analysis of the digested material and reached the value of 14.5 wt %, slightly lower than expected considering the quantity of iron chlorides and alumina used in the process (yield of iron deposition on alumina reaches 77.2 wt %). Accordingly, the efficiency of IO/Al_2O_3 for CVD measured as gram of CNT per gram of iron in IO/Al_2O_3, results in 11.1, 10.4 and 12.8 g/g for LDPE, HDPE and PP carbon precursor, respectively.

The remaining content in the PO-CNTs obtained from the CHNS-elemental analysis, as 100 wt %-C(wt %)-H(wt %)-N(wt %)-S(wt %), ranges values close to the ash content obtained by TGA, so oxygen or other heteroatoms in the PO-CNTs are considered negligible. The elemental composition values are similar to those found in the literature [33].

BET surface area (S_{BET}) and total pore volume (V_{Total}) of PO-CNTs were determined from N_2 adsorption isotherms at −196 °C. As observed, the values taken for S_{BET} and V_{Total} were found to be similar among them, ranging from 66 to 98 m^2 g^{-1} and 154–247 mm^3 g^{-1} for S_{BET} and V_{Total}, respectively. Apparently, the purification of the pristine CNTs does not affect the BET surface area, since close values were obtained between purified and non-purified CNTs (e.g. 66 m^2 g^{-1} for CNTW_LDPE and 67 m^2 g^{-1} for CNT_LDPE). Therefore, the metal content in the PO-CNTs, as IO/Al_2O_3 (S_{BET} = 139 m^2 g^{-1}), does not contribute to the BET surface area of the nanostructured carbon.

3.4. Magnetic properties

Fig. 5 shows photographs of CNTW_LDPE, CNTW_HDPE, and CNTW_PP in the absence (a-c) and the presence of a neodymium magnet (d̶ f̶e-g). As observed, the PO-CNTs have magnetic properties, due to the non-leached magnetic nanoparticles present inside the PO-CNTs after purification, which confer magnetic properties to the polyolefin-derived CNTs. To elucidate whether the magnetic properties were developed due to the thermal treatment at which iron nanoparticles are subjected during the growth of the CNTs, IO/Al_2O_3 was thermally treated under same conditions (850 °C for 1 h with N_2 flow of 50 mL min^{-1}). Fig. 6. d and.h show photographs of IO/Al_2O_3 before and after its thermal treatment at those conditions, evidencing that magnetic properties were developed just by the growth of the CNTs.

The metal substrate prepared for CCVD (IO/Al_2O_3) and a selected CNT (CNTW_LDPE) were ̶w̶a̶s̶ analyzed by XRD to identify crystal composition (Fig. 6). The analysis of IO/Al_2O_3 with the software X'Pert HighScore Plus allowed phase identification of alumina, hematite (α-Fe_2O_3), and magnetite (Fe_3O_4) based on reference cards 96–152–8248, 96–900–9783, and 96–900–6248, respectively (data obtained from Crystallography Open Database). Semi-quantitative analysis revealed that the metal substrate comprises 78 % alumina, 19 % hematite and 3 % magnetite. The high percentage of hematite was already expected due to the brown-red iron oxide color, along with the low magnetism observed visually for the CCVD substrate. In addition, the drying step of the metal substrate was performed in an ambient atmosphere, significantly increasing the oxidation of the material and reducing the chance of obtaining magnetite [50].

Despite the low magnetism observed for metal substrate, the CNTs recovered from the reactor had a great magnetic response, as shown in Fig. 5. The X-ray diffractograms of LDPE-derived CNTs (Fig. 6b) show the presence of graphite and cementite, the latter being responsible for the magnetic characteristics [51]. The semi-quantitative analysis resulted in 32 % and 19 % of cementite composition before and after purification with sulphuric acid, i.e. CNT_LDPE and CNTW_LDPE, respectively. The decrease in the content of cementite is expected due to
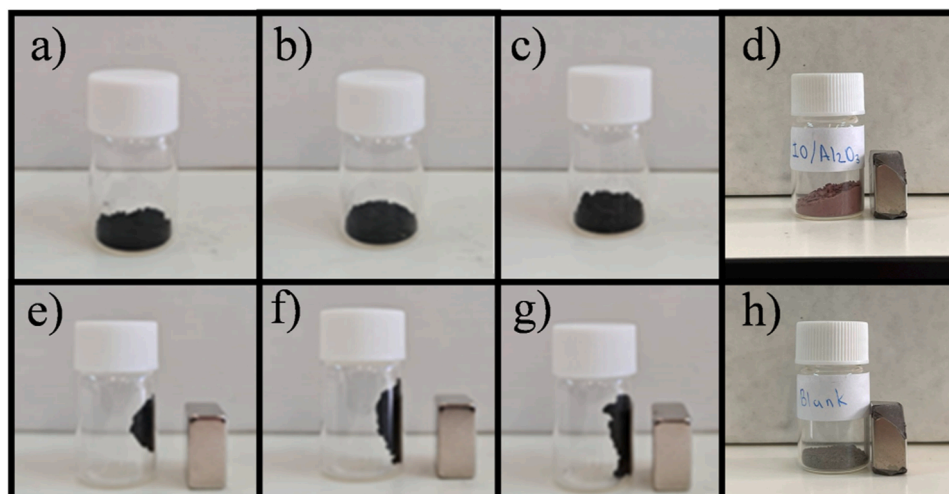

Fig. 5. Photographs of the PO-CNTs prepared from (a,d̶e) LDPE, (b,e̶f) HDPE and (c,f̶g) PP in the (a-c) absence and (d̶ f̶e-g) presence of neodymium magnet, (d) IO/Al$_2$O$_3$ and the iron oxide after its thermal treatment at same conditions than those used in the synthesis of CNTs.
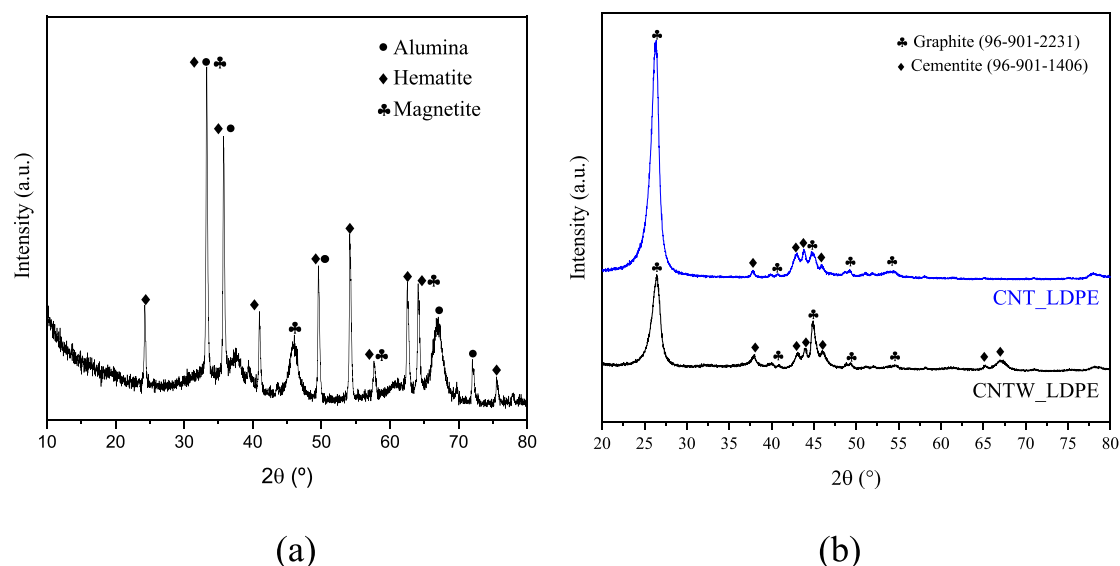
Fig. 6. X-ray diffractogram of (a) IO/Al$_2$O$_3$ and (b) CNT prepared from LDPE before and after purified with H$_2$SO$_4$.

metal-phase removal with the acid washing procedure. The phase change observed here from iron oxides to cementite was already reported in other studies and is related to hydrogen reduction faced by the metal substrate during the CVD process [52].

3.5. Application of the PO-CNTs in CWPO

3.5.1. Catalytic activity

The performance of the purified, ~~and~~ non-purified PO-CNTs and IO/Al$_2$O$_3$ as catalysts were assessed in the removal of paracetamol (PCM) by CWPO (Fenton-like system). The results in terms of removal of PCM, either by adsorption ($X_{PCM,ADS}$) or by CWPO ($X_{PCM,CWPO}$), abatement of TOC (X_{TOC}) and efficiency of hydrogen peroxide consumption (η_{H2O2}) using each PO-CNTs and IO/Al$_2$O$_3$ as catalyst after 6 h of reaction time are depicted in Fig. 7. Related to the removal of PCM by adsorption, purified CNT-catalysts (CNTW_LDPE, CNTW_HDPE, and CNTW_PP) allow to reach values ranging from 21.7 % to 31.8 %, which are higher than those observed with the non-purified PO-CNTs (11.5–14.8 %), despite the similar textural properties of purified and non-purified CNTs. This may be ascribed to the highest adsorption affinity of PCM for the purified CNTs, increasing the interaction between reactant and catalyst to accomplish higher conversions. In other words, as purified CNT have

higher carbon content (92.0–94.0 wt %) than non-purified catalysts (58.3–62.2 wt %), more active sites are available for PCM adsorption.

All materials were tested in both adsorption and CWPO at equal operating conditions ($C_{PCM,0}$ = 100 μg mL^{-1}, $C_{CNT catalyst}$ = 2.5 g L^{-1}, pH_0 = 3.5 and T = 80 °C) without adding H$_2$O$_2$ and with the addition of H$_2$O$_2$ ($C_{H2O2,0}$ = 472 μg mL^{-1}), respectively. As represented in Fig. 7, the removal of PCM by CWPO was higher (92.1–100 %) than the removal of PCM by adsorption with the same CNTs (11.5–31.8 %) or the removal by the non-catalytic run (X_{PCM} = 6.6 %), demonstrating the catalytic activity of the PO-CNTs. Furthermore, CNTs led to higher removals of PCM by CWPO than IO/Al$_2$O$_3$ catalyst, which was used in their growth, evidencing the greater catalytic activity of the CNT. In CWPO runs, TOC abatement was also measured after 6 h of reaction time. As noted, conversions of TOC reach values ranging from 41 % to 58 % for purified CNTs and 53–66 % for non-purified CNTs. That was ascribed to the higher content of iron in non-purified CNTs than the respective purified CNTs. All catalysts revealed stability against the leaching of iron species since the aliquots taken at the end of the oxidation experiments showed a negligible iron content (below the limit of detection of the equipment). Despite non-purified CNTs being stable and offering higher TOC conversions, using those catalysts results in an inefficient consumption of hydrogen peroxide, representing the highest
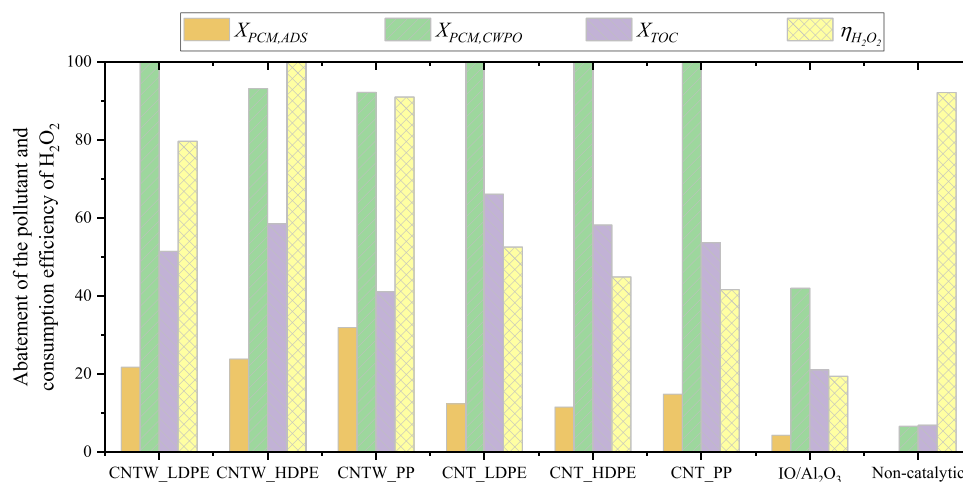

Fig. 7. Removal of paracetamol (PCM) from aqueous reaction media by adsorption and by CWPO; TOC removal, and H$_2$O$_2$ consumption efficiency obtained in the CWPO experiments; results after 6 h (Operating conditions: $C_{PCM,0}$ = 100 μg mL^{-1}, $C_{H2O2,0}$ = 472 μg mL^{-1}, $C_{catalyst}$ = 2.5 g L^{-1}, pH_0 = 3.5 and T = 80 °C).

operating cost in Fenton processes [42]. The efficiency of H_2O_2 consumption (η_{H2O2}), measured as TOC removal per H_2O_2 consumed in mols (Eq. (1)) reach values between 42 % and 52 % for non-purified CNTs, whereas purified CNTs allow operating with efficiencies higher than 80 % (this means that 80 % of hydrogen peroxide consumed allows degrading the organic matter in the process).

To the best of our knowledge, there is no other work dealing with the CWPO of PCM using CNTs, but it is possible to find studies about PCM degradation using other catalysts. In previous studies, pillared clays and carbon-coated nano-ferrites were assessed as catalysts in the CWPO of PCM at same operating conditions than those used in this work [40,53]. In both works, the catalyst presenting the best performance allows to reach the complete removal of PCM after only 6 h of reaction, thus, less catalytic activity was found compared to PO-CNTs. Velichkova et. al. [54] also achieved the complete removal of PCM after 4 h using a maghemite nanocatalyst and concentrations of 100 mg L^{-1}, 28 mmol L^{-1} and 6 g L^{-1} for paracetamol, hydrogen peroxide and catalyst, respectively, so higher dose of H_2O_2 and loads of catalysts were used compared to this work. Hachemaoui et al. report complete removals of PCM after 0.5 h using chromium supported on MCM-41 as catalysts, but the initial concentration of the model micropollutant was considerably lower (5 µg mL^{-1}) than in this work and similar catalysts loads were used (2 g L^{-1}) [55]. Carrasco-Díaz et al. report the use of iron-carbon xerogels as catalysts for the degradation of PCM by H_2O_2. The catalysts allowed reaching 90 % of PCM removal after 1 h of reaction using 50 µg mL^{-1} as the initial concentration of PCM, 25 ºC, pH 3 and 13.8 mM of H_2O_2 (higher than the stoichiometric quantity for the complete oxidation of PCM) [56]. In papers related to Fenton process, complete removals of PCM were achieved after 1 h at similar operating conditions than those used in this work [57,58]; however, the use of an homogeneous catalyst needs an additional process to recover the catalyst. In this study, the magnetic CNTs can be easily recovered in several ways, including using of magnetic field.

3.5.2. Conversion profiles with purified PO-CNTs

The concentration profiles were monitored during CWPO runs to investigate the PCM, and H_2O_2 concentrations, as well as the removal in terms of aromatic (X_{AROM}) and total phenolic compounds ($X_{phenols}$), using selected PO-CNTs (purified materials: CNTW_LDPE, CNTW_HDPE, and CNTW_PP). The conversions of PCM, H_2O_2, aromatic and total phenolic compounds are depicted in Fig. 8. As observed, all catalysts present similar conversion profiles. Hydrogen peroxide does not reach its half conversion at 6 h of reaction time, showing a controlled consumption of the reagent, which is interesting taking into account that hydrogen peroxide constitutes the highest operating cost in Fenton-like processes [59]. CNTW_LDPE shows a slightly higher catalytic activity, allowing to convert more than 80 % of PCM in half an hour and to reach complete removal of PCM after 4 h of reaction with this sample of CNTs. In a previous work, we studied the removal of PCM in the presence of pillared clays as catalysts at equal conditions (same catalyst, hydrogen peroxide and PCM concentration, pH, and temperature) [40]. For the complete removal of PCM, more than 6 h of reaction was required, evidencing that CNTW_LDPE has the potential to act as a catalyst in the removal of organic pollutants in water matrix solutions by CWPO.

Curve profiles for the total phenolic compounds determined by FCR (Fig. 8.b) were found to be similar to curve profiles of PCM, since complete conversion is achieved in 4 h of reaction. However, aromatic compounds present a slower conversion profile compared to total phenolic and PCM removals, evidencing that oxidized intermediates are formed during the process, as expected by considering the TOC results (Fig. 7). Removing the contribution of PCM to the absorbance of aromatic compounds, it is possible to determine removals higher than 67 % of aromatics from 6 to 24 h of reaction.

3.5.3. Stability of PO-CNT

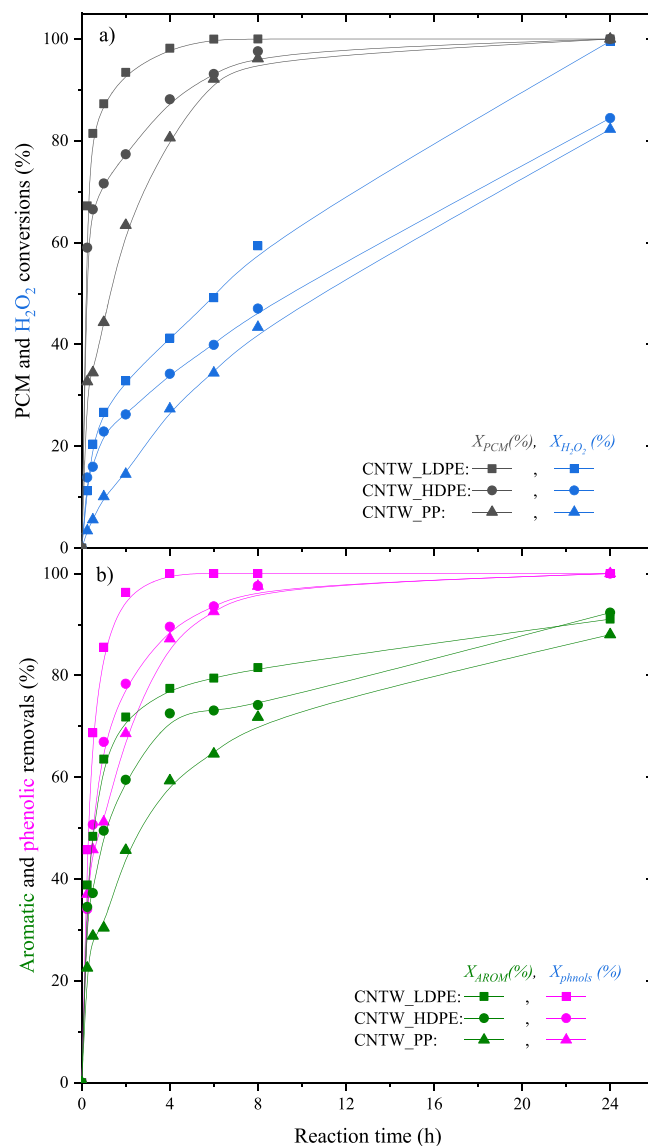The stability of the PO-CNT has been studied through two

Fig. 8. Profiles upon reaction time of (a) PCM and H_2O_2 conversions and removals of (b) aromatic and total phenolic compounds in the CWPO experiments performed under the following conditions: $C_{PCM,0} = 100$ µg mL^{-1}, $C_{H2O2,0} = 472$ µg mL^{-1}, $C_{cat} = 2.5$ g L^{-1}, $pH_0 = 3.5$ and T = 80 °C.

approaches: 1) assessing the existence of poisoning of CNTW_LDPE by the presence of the micro-pollutant before being used in CWPO, and 2) evaluating the reusability of the same CNT as a catalyst in CWPO in three consecutive runs. For the first hypothesis, a suspension of CNTW_LDPE with PCM at the same operating conditions than those used in CWPO experiments ($C_{PCM,0} = 100$ µg mL^{-1}, $C_{catalyst} = 2.5$ g L^{-1}, $pH_0 = 3.5$ and T = 80 °C) was stirred during 48 h. Then, hydrogen peroxide was added ($C_{H2O2,0} = 472$ µg mL^{-1}) and CWPO was monitored upon reaction time for 24 h. In Fig. 9, the relative concentration profile of PCM upon reaction is compared to the CWPO of PCM with CNTW_LDPE at the typical operating conditions previously used and with an oxidation run without catalyst. As observed, preliminary adsorption of the micropollutant on CNTW_LDPE does not hinders the oxidation of PCM and the catalyst maintains the same catalytic activity.

The reusability of the magnetic polyolefins-derived CNTs as a catalyst in CWPO was studied using CNTW_LDPE material in three consecutive runs (after each experiment, CNTW_LDPE was recovered by filtration, washed with distilled water, dried, weighted and used in a successive experiment). Fig. 10 shows the relative concentration profile
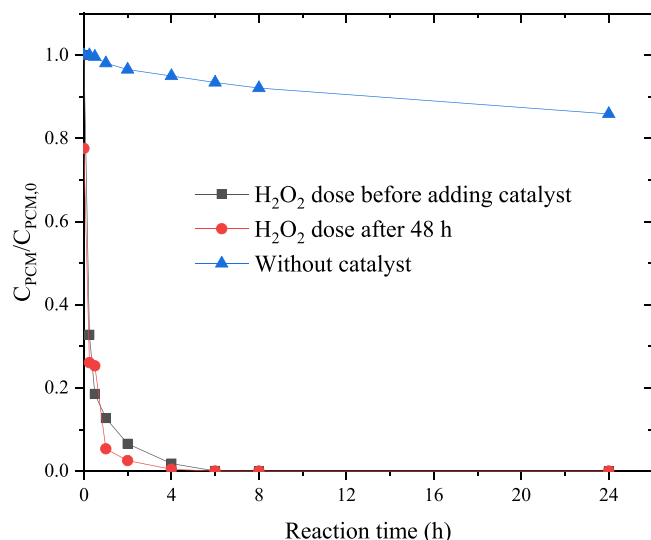
Fig. 9. Effect of preliminary adsorption of PCM prior to CWPO with CNTW_LDPE catalyst under the following conditions: $C_{PCM,0} = 100\ \mu g\ mL^{-1}$, $C_{H2O2,0} = 472\ \mu g\ mL^{-1}$, $C_{cat} = 2.5\ g\ L^{-1}$, $pH_0 = 3.5$ and T = 80 °C.
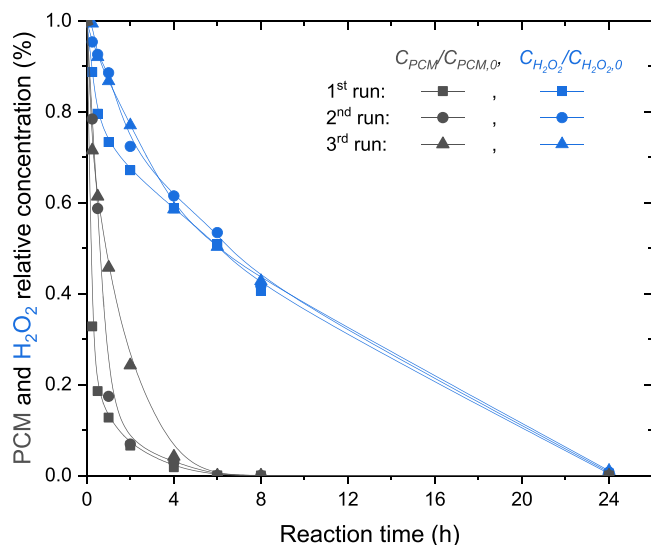

Fig. 10. PCM and H_2O_2 relative concentration profiles upon reaction time after reutilization runs with CNTW_LDPE catalyst under the following conditions: $C_{PCM,0} = 100\ \mu g\ mL^{-1}$, $C_{H2O2,0} = 472\ \mu g\ mL^{-1}$, $C_{cat} = 2.5\ g\ L^{-1}$, $pH_0 = 3.5$ and T = 80 °C.

of PCM and H_2O_2 upon CWPO time under the same operating conditions. As observed, the successive use of the CNTW_LDPE as a catalyst led to a partial decrease of its catalytic activity in the CWPO of PCM. After 4 h of reaction, 41.2 %, 38.5 % and 41.4 % of H_2O_2 consumptions were reached in the first, second and third uses of CNTW_LDPE. Moreover, PCM removals of 98.2 %, 97.1 % and 95.9 % are achieved in the first, second and third cycles with this catalyst, demonstrating the reusability of magnetic polyolefins-derived CNTs in the CWPO process for water treatment.

The deactivation is more evident with other catalysts applied in the catalytic wet peroxide oxidation. In a previous work dealing with the preparation of hydrochars from malt bagasse with catalytic activity, a reduction of the catalytic activity was observed from the first to the second CWPO run, leading to slightly less removal of caffeine (71 % after 1 h of reaction in the second run, whereas 92 % is obtained in the first run). The decrease in the catalytic activity of the material was ascribed

to changes in the superficial functional groups during the oxidation with hydrogen peroxide [2].

Martin-Martinez et al. studied the CWPO of 4-nitrophenol using different carbon nanotubes as catalysts and assessed the reusability of a carbon nanotube in three consecutive CWPO cycles [35]. The results show a high loss of catalytic activity since ca. 92 % of the model pollutant was removed after eight hours of reaction time in the first use of the catalyst. In contrast, whereas a pollutant removal of 21 % and 13 % was achieved in the second and third uses of the catalyst at the same reaction time.

Pinho et al. also reported consecutive uses of commercial carbon nanotubes in the CWPO of phenol [60]. The carbon nanotubes, which show the highest catalytic activity, were those produced with iron particles in the growth of the carbon nanotubes by chemical vapour deposition. However, the leaching of iron was evident, since iron concentration up to 2 mg L^{-1} was determined in the effluent of the CWPO process. Consequently, a slight loss of catalytic activity for those carbon nanotubes was observed in consecutive uses.

The use of magnetite supported on CNT for the CWPO of diclofenac, used as a model pollutant, has been reported by Huaccallo-Aguilar et al. [27]. The reusability of the catalyst was also explored and a loss of catalytic activity was evidenced since diclofenac removals of ca. 52 %, 43 % and 24 % were achieved in the first, second and third runs with the catalyst.

More recently, Huang et al. reported the application of a catalyst consisting of Fe$_3$C nanocrystal encapsulated CNT [61]. The reuse of the catalyst shows a slight increment of the catalytic activity in its use since phenol conversion increased from 83 % in the first cycle to 92 % in the fourth one. This may be ascribed to the changes on the surface of carbon materials used in an oxidation environment (as in CWPO), increasing the catalytic activity of the carbon catalyst, as reported in a previous work for the CWPO of phenol with carbon black [62].

4. Conclusions

In this work, we proposed a route for manufacturing magnetic catalysts tailored to the CWPO of PCM. The process is based on the valorization of polyolefins through synthesizing carbon nanotubes via CCVD, constituting a benefit in the long-term management of plastic wastes.

Using a one-chamber reactor, in which polymer cracking and CCVD happen at the same compartment, this approach might limit control over the overall conditions of polymer cracking and deposition mechanism but represents one alternative to decrease resource expenses and increase the feasibility of the process.

Although CNTs are known for their applicability in a diverse range of electronic device, their use in environmental chemistry still has room for improvement. Here we showed that CNTs have potential applications as catalysts for the CWPO of organic pollutants. In the circumstance of PCM being wholly removed from a simulated matrix within 6 h of reaction. The utilization of carbon-based materials in this technology represents a solution to the problem of iron leaching faced by the utilization of typical catalysts (i.e., metal phase over support).

The work reported here can be of particular interest to scholars trying to find solutions to tackle two environmental problems: plastic upcycling strategies and organic pollutants' presence in water bodies. The solution we presented here has the potential to be explored in different systems, considering other contaminants of interest and investigating the performance to treat wastewater. Additionally, the synthesis of CNTs using metal substrates prepared by sol-gel represents one route that can overcome higher yields of carbonaceous materials since the synthesis procedure ensures high purity metals supported on alumina. Moreover, other feedstock compositions could be explored to synthesize CNTs, to assess the possibility of valorizing other polymer streams.

CRediT authorship contribution statement

Jose L. Diaz de Tuesta: Conceptualization, Methodology, Formal analysis, Writing - Original draft preparation, Supervision, Visualization, Funding acquisition, Project administration. **Adriano S. Silva**: Investigation, Formal analysis, Validation, Writing - Reviewing and Editing. **Fernanda F. Roman**: Investigation, Formal analysis, Writing - Reviewing and Editing, **Lucas F. Sanches**: Investigation, Writing - Original draft preparation. **Fernando Alves da Silva**: Supervision, Writing - Reviewing and Editing. **Ana I. Pereira**: Supervision, Writing-Reviewing and Editing. **Adrián M.T. Silva**: Supervision, Writing-Reviewing and Editing, Funding acquisition, Project administration. **Joaquim L. Faria**: Supervision, Writing - Reviewing and Editing, **Helder T. Gomes**: Supervision, Conceptualization, Writing - Reviewing and Editing, Funding acquisition, Project administration.

Declaration of Competing Interest

The authors declare that they have no known competing financial interests or personal relationships that could have appeared to influence the work reported in this paper.

Data availability

No data was used for the research described in the article.

Acknowledgments

References

[1] X. Yuan, P.D. Dissanayake, B. Gao, W.J. Liu, K.B. Lee, Y.S. Ok, J. Environ. Manag. 296 (2021), 113128.
[2] J.L. Diaz de Tuesta, M.C. Saviotti, F.F. Roman, G.F. Pantuzza, H.J.F. Sartori, A. Shinibekova, M.S. Kalmakhanova, B.K. Massalimova, J.M.T.A. Pietrobelli, G. G. Lenzi, H.T. Gomes, J. Environ. Chem. Eng. 9 (2021), 105004.
[3] G. de Freitas Batista, F.F. Roman, J.L. Diaz de Tuesta, R.V. Mambrini, P. Praça, H. T. Gomes, Catalysts 12 (2022) 238.
[4] Z. Chen, W. Wei, B.-J. Ni, H. Chen, Environ. Funct. Mater. 1 (2022) 34–48.
[5] S. Chen, Z. Liu, S. Jiang, H. Hou, Sci. Total Environ. 710 (2020), 136250.
[6] X. Chen, Y. Wang, L. Zhang, ChemSusChem 14 (2021) 4137–4151.
[7] A. Bazargan, G. McKay, Chem. Eng. J. 195–196 (2012) 377–391.
[8] C. Zhuo, Y.A. Levendis, J. Appl. Polym. Sci. 131 (2014) 39931 (39931-39914).
[9] O. Vieira, R.S. Ribeiro, J.L. Diaz de Tuesta, H.T. Gomes, A.M.T. Silva, Chem. Eng. J. 428 (2022), 131399.
[10] W. Mai, B. Sun, L. Chen, F. Xu, H. Liu, Y. Liang, R. Fu, D. Wu, K. Matyjaszewski, J. Am. Chem. Soc. 137 (2015) 13256–13259.
[11] J. Gong, X. Chen, T. Tang, Prog. Polym. Sci. 94 (2019) 1–32.
[12] V.G. Pol, M.M. Thackeray, Energy Environ. Sci. 4 (2011) 1904–1912.
[13] X. Wen, X. Chen, N. Tian, J. Gong, J. Liu, M.H. Rümmeli, P.K. Chu, E. Mijiwska, T. Tang, Environ. Sci. Technol. 48 (2014) 4048–4055.
[14] L. Gao, F. Zhou, Q. Chen, G. Duan, ChemistrySelect 3 (2018) 5321–5325.
[15] J.G.S. Moo, A. Veksha, W.-D. Oh, A. Giannis, W.D.C. Udayanga, S.-X. Lin, L. Ge, G. Lisak, Electrochem. Commun. 101 (2019) 11–18.
[16] N. Cai, S. Xia, X. Zhang, Z. Meng, P. Bartocci, F. Fantozzi, Y. Chen, H. Chen, P. T. Williams, H. Yang, ChemSusChem 13 (2020) 938–944.
[17] A. Veksha, K. Yin, J.G.S. Moo, W.-D. Oh, A. Ahamed, W.Q. Chen, P. Weerachanchai, A. Giannis, G. Lisak, J. Hazard. Mater. 387 (2020) 121256.
[18] N. Cai, H. Yang, X. Zhang, S. Xia, D. Yao, P. Bartocci, F. Fantozzi, Y. Chen, H. Chen, P.T. Williams, Waste Manag. 109 (2020) 119–126.
[19] V. Sridhar, H. Park, Materials 13 (2020) 4144.
[20] J. Gong, J. Liu, X. Chen, Z. Jiang, X. Wen, E. Mijowska, T. Tang, RSC Adv. 4 (2014) 33806–33814.
[21] S.K. Deokar, G.S. Bajad, P. Bhonde, R.P. Vijayakumar, S.A. Mandavgane, J. Polym. Environ. 25 (2017) 165–175.
[22] N. Borsodi, A. Szentes, N. Miskolczi, C. Wu, X. Liu, J. Anal. Appl. Pyrolysis 120 (2016) 304–313.
[23] C. Wu, M.A. Nahil, N. Miskolczi, J. Huang, P.T. Williams, Process Saf. Environ. Prot. 103 (2016) 107–114.
[24] A. Mezni, N.B. Saber, A.A. Alhadhrami, A. Gobouri, A. Aldalbahi, S. Hay, A. Santos, D. Losic, T. Altalhi, J. Drug, Deliv. Sci. Technol. 41 (2017) 351–358.
[25] G. Ovejero, J.L. Sotelo, M.D. Romero, A. Rodríguez, M.A. Ocaña, G. Rodríguez, J. García, Ind. Eng. Chem. Res 45 (2006) 2206–2212.
[26] Y. Huaccallo-Aguilar, S. Álvarez-Torrellas, M. Larriba, V.I. Águeda, J.A. Delgado, G. Ovejero, J. García, Catalysts 9 (2019) 287.
[27] Y. Huaccallo-Aguilar, S. Álvarez-Torrellas, J. Martínez-Nieves, J. Delgado-Adámez, M.V. Gil, G. Ovejero, J. García, Catalysts 11 (2021) 514.
[28] Y. Huaccallo-Aguilar, J.L. Diaz de Tuesta, S. Álvarez-Torrellas, H. Teixeira Gomes, M. Larriba, G. Ovejero, J. García, J. Environ. Manag. 281 (2021), 111913.
[29] R.S. Ribeiro, O. Vieira, R. Fernandes, F.F. Roman, J.L. Diaz de Tuesta, A.M.T. Silva, H.T. Gomes, J. Environ. Manag. 308 (2022), 114622.
[30] R.S. Ribeiro, A.M.T. Silva, J.L. Figueiredo, J.L. Faria, H.T. Gomes, Appl. Catal. B 187 (2016) 428–460.
[31] J.L. Diaz de Tuesta, A. Quintanilla, J.A. Casas, S. Morales-Torres, J.L. Faria, A.M. T. Silva, H.T. Gomes, Catal. Today 356 (2020) 216–225.
[32] J.L. Diaz de Tuesta, F.V.M. de Almeida, J.R.P. Oliveira, P. Praça, M.C. Guerreiro, H. T. Gomes, Environ. Tech. Innov. 24 (2021), 101984.
[33] J.L. Diaz de Tuesta, B.F. Machado, P. Serp, A.M.T. Silva, J.L. Faria, H.T. Gomes, Catal. Today 356 (2020) 205–215.
[34] Y. Huaccallo, S. Alvarez-Torrellas, M.P. Marin, M.V. Gil, M. Larriba, V.I. Agueda, G. Ovejero, J. Garcia, Environ. Sci. Pollut. Res. Int. 26 (2019) 22372–22388.
[35] M. Martin-Martínez, R.S. Ribeiro, B.F. Machado, P. Serp, S. Morales-Torres, A.M. T. Silva, J.L. Figueiredo, J.L. Faria, H.T. Gomes, ChemCatChem 8 (2016) 2068–2078.
[36] M. Martin-Martinez, B.F. Machado, P. Serp, S. Morales-Torres, A.M.T. Silva, J. L. Figueiredo, J.L. Faria, H.T. Gomes, Catal. Today 357 (2020) 332–340.
[37] Y. Huaccallo-Aguilar, S. Álvarez-Torrellas, M. Larriba, V.I. Águeda, J.A. Delgado, G. Ovejero, J.A. Peres, J. García, J. Environ. Chem. Eng. 9 (2021), 105110.
[38] J.L. Diaz De Tuesta, F.F. Roman, V.C. Marques, A.S. Silva, A.P.F. Silva, T.C. Bosco, A.A. Shinibekova, S. Aknur, M.S. Kalmakhanova, B.K. Massalimova, M. Arrobas, A. M.T. Silva, H.T. Gomes, J. Environ. Chem. Eng. 10 (2022), 108143.
[39] J. Cardoso, H.T. Gomes, P. Brito, Recycling 4 (2019) 8.
[40] A. Santos Silva, M. Seitovna Kalmakhanova, B. Kabykenovna Massalimova, J. G. Sgorlon, J.L. Diaz de Tuesta, H.T. Gomes, Catalysts 9 (2019) 705.
[41] J.D. Box, Water Res 17 (1983) 511–525.
[42] J.L. Diaz de Tuesta, A. Quintanilla, D. Moreno, V.R. Ferro, J.A. Casas, Catalysts 10 (2020) 548.
[43] J. Gong, J. Feng, J. Liu, R. Muhammad, X. Chen, Z. Jiang, E. Mijowska, X. Wen, T. Tang, Ind. Eng. Chem. Res. 52 (2013) 15578–15588.
[44] J. Gong, J. Feng, J. Liu, Z. Jiang, X. Chen, E. Mijowska, X. Wen, T. Tang, Chem. Eng. J. 248 (2014) 27–40.
[45] V.G. Pol, P. Thiyagarajan, J. Environ. Monit.: JEM 12 (2010) 455–459.
[46] J. Zhang, J. Li, J. Cao, Y. Qian, Mater. Lett. 62 (2008) 1839–1842.
[47] L.S.K. Pang, J.D. Saxby, S.P. Chatfield, J. Phys. Chem. 97 (1993) 6941–6942.
[48] C.E. Johnson, W.A. Weimer, D.C. Harris, Mater. Res. Bull. 24 (1989) 1127–1134.
[49] F. Farivar, P. Lay Yap, R.U. Karunagaran, D. Losic, C 7 (2021) 41.
[50] J. Xu, H. Yang, W. Fu, K. Du, Y. Sui, J. Chen, Y. Zeng, M. Li, G. Zou, J. Magn. Magn. Mater. 309 (2007) 307–311.
[51] D. Chaira, B.K. Mishra, S. Sangal, J. Alloy. Compd. 474 (2009) 396–400.
[52] A.A.S. Oliveira, I.F. Teixeira, T. Christofani, J.C. Tristão, I.R. Guimarães, F.C. C. Moura, Appl. Catal. B 144 (2014) 144–151.
[53] N.M.C. Guari, A.S. Silva, J.L. Diaz de Tuesta, W.E. Pottker, P.Y. Cordeiro, H. T. Gomes, Glob. NEST J. 24 (2022) 1–10.
[54] F. Velichkova, C. Julcour-Lebigue, B. Koumanova, H. Delmas, J. Environ. Chem. Eng. 1 (2013) 1214–1222.
[55] M. Hachemaoui, C.B. Molina, C. Belver, J. Bedia, A. Mokhtar, R. Hamacha, B. Boukoussa, Catalysts 11 (2021) 219.
[56] M.R. Carrasco-Díaz, E. Castillejos-López, A. Cerpa-Naranjo, M.L. Rojas-Cervantes, Micro Mesop. Mater. 237 (2017) 282–293.
[57] M.G. Alalm, A. Tawfik, S. Ookawara, J. Environ. Chem. Eng. 3 (2015) 46–51.
[58] A.G. Trovó, R.F. Pupo Nogueira, A. Agüera, A.R. Fernandez-Alba, S. Malato, Water Res. 46 (2012) 5374–5380.
[59] J.L. Díaz de Tuesta, C. García-Figueruelo, A. Quintanilla, J.A. Casas, J.J. Rodriguez, J. Chem. Technol. Biotechnol. 90 (2015) 1839–1846.
[60] M.T. Pinho, H.T. Gomes, R.S. Ribeiro, J.L. Faria, A.M.T. Silva, Appl. Catal. B 165 (2015) 706–714.
[61] H. Huang, H. Zhang, Y. Yan, J. Hazard Mater. 407 (2021), 124371.
[62] J.L. Diaz de Tuesta, A. Quintanilla, J.A. Casas, J.J. Rodriguez, Appl. Catal. B 209 (2017) 701–710.